

Non-Fermi-Liquid Behavior in Metallic Quasicrystals with Local Magnetic Moments

Eric C. Andrade,¹ Anuradha Jagannathan,² Eduardo Miranda,³ Matthias Vojta,⁴ and Vladimir Dobrosavljević⁵

¹*Instituto de Física Teórica, Universidade Estadual Paulista,*

Rua Dr. Bento Teobaldo Ferraz, 271 - Bloco II, 01140-070, São Paulo, SP, Brazil

²*Laboratoire de Physique des Solides, CNRS-UMR 8502, Université Paris-Sud, 91405 Orsay, France*

³*Instituto de Física Gleb Wataghin, Unicamp, Rua Sérgio Buarque de Holanda, 777, CEP 13083-859 Campinas, SP, Brazil*

⁴*Institut für Theoretische Physik, Technische Universität Dresden, 01062 Dresden, Germany*

⁵*Department of Physics and National High Magnetic Field Laboratory,
Florida State University, Tallahassee, Florida 32306, USA*

(Dated: October 23, 2018)

Motivated by the intrinsic non-Fermi-liquid behavior observed in the heavy-fermion quasicrystal $\text{Au}_{51}\text{Al}_{34}\text{Yb}_{15}$, we study the low-temperature behavior of dilute magnetic impurities placed in metallic quasicrystals. We find that a large fraction of the magnetic moments are not quenched down to very low temperatures T , leading to a power-law distribution of Kondo temperatures $P(T_K) \sim T_K^{\alpha-1}$, with a non-universal exponent α , in a remarkable similarity to the Kondo-disorder scenario found in disordered heavy-fermion metals. For $\alpha < 1$, the resulting singular $P(T_K)$ induces non-Fermi-liquid behavior with diverging thermodynamic responses as $T \rightarrow 0$.

PACS numbers: 71.10.Hf, 71.23.Ft, 75.20.Hr

Introduction.—Fermi-liquid (FL) theory forms the basis of our understanding of interacting fermions. It works in a broad range of systems, from weakly correlated metals [1] to strongly interacting heavy fermions [2]. Over the past decades, however, the properties of numerous metals have been experimentally found to deviate from FL predictions [3, 4], and much effort has been devoted to the understanding of such non-Fermi-liquid (NFL) behavior. One interesting avenue is provided by quantum critical points (QCPs): NFL physics may occur in the associated quantum critical regime which is reached upon tuning the system via a nonthermal control parameter such as pressure, doping, or magnetic field [5, 6].

Remarkably, recent experiments have provided compelling evidence of NFL behavior without fine-tuning in the heavy-fermion *quasicrystal* $\text{Au}_{51}\text{Al}_{34}\text{Yb}_{15}$ [7, 8]. Furthermore, Ref. 7 also reports that no NFL behavior emerges when one considers a crystalline approximant instead of the quasicrystal, suggesting that this NFL regime is associated with the particular electronic states present in the quasicrystal but not in the approximant [9–14]. Conventional QCP approaches have been employed to explain the fascinating behavior in this alloy [15, 16], but they consider the effects of quasicrystalline environment of the conduction electrons only minimally.

In this work we intend to close this gap by presenting a detailed calculation of the fate of isolated localized magnetic moments when placed in both two- and three-dimensional quasicrystals. Our results for dilute impurities show that a considerable fraction of impurity moments is not quenched down to very low temperatures, leading to a power-law distribution of Kondo temperatures, $P(T_K) \propto T_K^{\alpha-1}$, with a nonuniversal exponent α . This results in NFL behavior in both χ and C/T as $T \rightarrow 0$: $\chi \sim C/T \sim T^{\alpha-1}$ [17], a scenario very remi-

niscient of the Kondo effect in disordered metals [18–23]. Moreover, we show that the strong energy dependence of the electronic density of states (DOS) characteristic of a quasicrystal leads to a situation such that small changes in the model parameters (band filling, Kondo coupling, etc.) may drive the system in and out of the NFL region.

Quasicrystalline wave functions.—A quasicrystal exhibits a small set of local environments, which reappear again and again, albeit not in a periodic fashion. Their pattern is not random either, since the structure factor shows sharp Bragg peaks, although their symmetry is noncrystallographic [24]. The n -fold symmetries (with values of $n = 5, 8, 10, \dots$) seen in the diffraction pattern of quasicrystals arise due to the fact that the local environments occur with n equiprobable orientations.

The structure factor of quasicrystals is densely filled in reciprocal space with diffraction spots [24] of widely differing intensities. The brighter peaks are expected to lead to strong scattering of conduction electrons, giving rise to spikes in the DOS [25, 26]. The scattering due to the remaining peaks, while weaker, results in wave functions which show fluctuations at all length scales. The Fibonacci chain, a one-dimensional quasicrystal, provides an example of such wave functions [9], often referred to as *critical* [9–13], in analogy with those found at the Anderson metal-insulator transition [27, 28].

Tiling model.—For simplicity, we consider models on quasiperiodic tilings. We first report results obtained for a 2D tiling, where it is easier to handle large system sizes numerically. In the Supplemental Material [29], we show calculations for a 3D tiling [30] with very similar results, confirming that our scenario is independent of both tiling details and dimensionality.

The 2D tiling we consider is the octagonal tiling (Ammann-Beenker) [31], Fig. 1(a). This tiling is com-

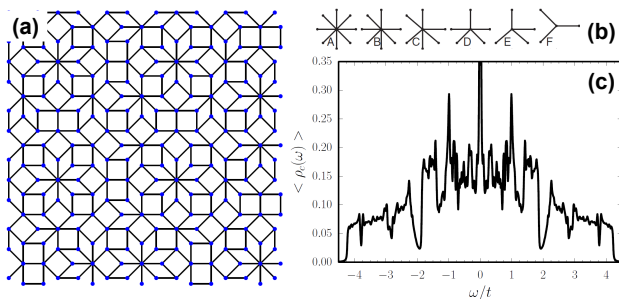


Figure 1: Quasicrystal geometrical and electronic properties. (a) Square approximant for the perfect octagonal tiling with $N_a = 239$ sites. (b) The six local site environments with $z = 3, \dots, 8$ nearest neighbors. (c) The total DOS as a function of the energy for the $N_a = 8119$ approximant averaged over $N_\phi = 64$ twist angles.

posed of two types of decorated tiles: squares and 45° rhombuses, which combine to create six distinct local environments with coordination number $z = 3, \dots, 8$, Fig. 1(b).

As a minimal model to describe the electronic properties of quasicrystals, we consider a nearest-neighbor tight-binding Hamiltonian in standard notation

$$\mathcal{H}_c = -t \sum_{\langle ij \rangle, \sigma} (c_{i\sigma}^\dagger c_{j\sigma} + c_{j\sigma}^\dagger c_{i\sigma}). \quad (1)$$

In the following, energies are measured in units of t . In our calculation, we consider periodic approximants of the octagonal tiling of sizes $N_a = 7, 41, 239, 1393$, and 8119 , obtained by the standard method of projecting down from a higher dimensional cubic lattice, as in previous works [31–34]. To reduce finite-size effects we use twisted boundary conditions, i.e., $\psi(\vec{r} + L\hat{x} + L\hat{y}) = e^{i\phi_x} e^{i\phi_y} \psi(\vec{r})$ for a sample of linear size L . Our final answer is obtained averaging over N_ϕ twist angles [35].

In Fig. 1(c) we show the well-known total DOS for the octagonal tiling $\langle \rho_c(\omega) \rangle = \sum_{i=1}^{N_a} \rho_i^c(\omega) / N_a$, with the local DOS at site i given by $\rho_i^c(\omega) = \sum_\nu |\psi_\nu^c(i)|^2 \delta(\omega - E_\nu^c)$, where ψ_ν^c is an eigenstate of \mathcal{H}_c in (1) with energy E_ν^c and the overline denotes the average over boundary conditions. $\langle \rho_c(\omega) \rangle$ has a strong energy dependence with several spikes and a pronounced dip at $\omega \approx \pm 2.0t$. The large peak at $\omega = 0$ is due to families of strictly localized states, a consequence of the local topology of the octagonal tiling [12, 36]. The spatial structure of $\rho_i^c(\omega)$ is discussed in Ref. [29], where we show that it is well described by a log-normal distribution.

Local moments and large- N solution.—We now move to the main topic of this Letter: the investigation of the single-impurity Kondo effect in a metallic quasicrystal. Specifically, we consider the $U \rightarrow \infty$ Anderson impurity

model

$$\mathcal{H} = \mathcal{H}_c + E_f \sum_\sigma n_{f\sigma} + V \sum_\sigma (f_{\ell\sigma}^\dagger c_{\ell\sigma} + c_{\ell\sigma}^\dagger f_{\ell\sigma}). \quad (2)$$

This model describes a band of noninteracting electrons (c band) which hybridize with a localized f orbital located at site ℓ . The operator $f_{\ell\sigma}^\dagger$ ($f_{\ell\sigma}$) creates (destroys) an electron with spin σ at the impurity site ℓ and the $U \rightarrow \infty$ limit imposes the constraint $n_{f\sigma} = f_{\ell\sigma}^\dagger f_{\ell\sigma} \leq 1$. E_f is the f -level energy, measured with respect to the chemical potential μ , and the hybridization V couples the impurity site to the conduction band. To obtain quantitative results, we now turn to a large- N limit of Eq. (2) that allows us to access arbitrary values of the model parameters [37–39]. It introduces two variational parameters Z_ℓ (quasiparticle weights) and $\tilde{\epsilon}_{f\ell}$ (renormalized f -energy levels), which are site dependent in the case of a quasicrystal. These parameters are determined by minimization of the saddle-point free energy (see [29] for further details)

$$F_{MF}^\ell = \frac{2}{\pi} \int_{-\infty}^{+\infty} f(\omega) \text{Im} \left[\ln \left[\tilde{G}_\ell^f(\omega) \right] \right] d\omega + (\tilde{\epsilon}_{f\ell} - E_f) (Z_\ell - 1), \quad (3)$$

where $f(\omega)$ is the Fermi-Dirac distribution function. The quasiparticle f -level Green’s function is given by $\tilde{G}_\ell^f(\omega) = [\omega - \tilde{\epsilon}_f - Z_\ell \Delta_{f\ell}(\omega)]^{-1}$, with the f -electron hybridization function given by $\Delta_{f\ell}(\omega) = V^2 G_{\ell\ell}^c(\omega)$, where $G_{\ell\ell}^c(\omega) = \sum_\nu |\psi_\nu^c(\ell)|^2 / (\omega - E_\nu^c)$ is the c -electron Green’s function. We define T_K as the (half-)width of the resonance at the Fermi level $T_K^\ell \equiv Z_\ell \text{Im} [\Delta_{f\ell}(0)]$ [40] and introduce the Kondo coupling $J \equiv 2V^2 / |E_f|$. The f -level occupation is simply given by $n_{f\ell} = 1 - Z_\ell$.

Because each site in the quasicrystal “sees” a different environment, encoded in $\Delta_{f\ell}(\omega)$, we numerically solve Eq. (3), at $T = 0$, individually placing Kondo impurities at all N_a sites of the approximant. Therefore, for every single impurity problem we obtain a different value of T_K , which we use to construct the distribution of the Kondo temperatures $P(T_K)$.

Power-law distribution of Kondo temperatures.—For Kondo impurities placed in a disordered metal [18–23] it is well established that the distribution of Kondo temperatures possesses a power-law tail at low T_K : $P(T_K) \propto T_K^{\alpha-1}$, with a nonuniversal exponent α [41]. For $\alpha < 1$, $P(T_K)$ becomes singular, and NFL behavior emerges in the system [17, 29].

Surprisingly, we observe the same phenomenology for quasicrystals, with sample results shown in Fig. 2. Here we show the corresponding $P(T_K)$ for the octagonal tiling at $\mu = -2.2t$ as a function of T_K / T_K^{typ} (we defined the typical value of T_K as $T_K^{\text{typ}} \equiv \exp[\langle \ln(T_K) \rangle]$). For approximants with $N_a \geq 239$ a clear power-law tail emerges for $T_K < T_K^{\text{typ}}$ with an exponent which depends on the

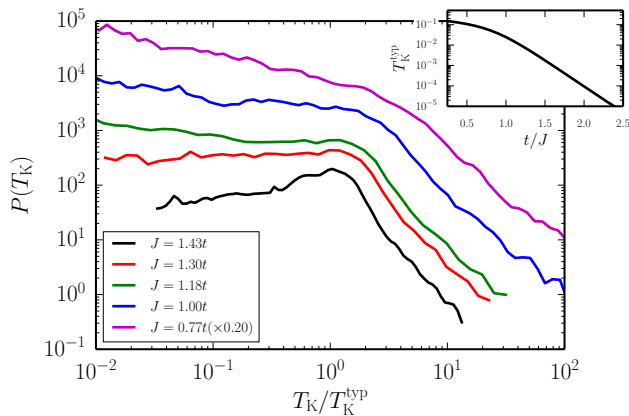


Figure 2: Distribution of the local Kondo temperatures $P(T_K)$ on a log-log scale for several values of the Kondo coupling J ; note that the curve corresponding to $J = 0.77t$ was scaled down. T_K on the horizontal axis has been normalized by T_K^{typ} ; the unrenormalized distributions are shown in Ref. 29. For $T_K \lesssim T_K^{\text{typ}}$ the distributions acquire a power-law form $P(T_K) \sim T_K^{\alpha-1}$, with the exponent α continuously varying with J . For $\alpha < 1$ the distribution is singular. (Notice that for $T_K \gtrsim T_K^{\text{typ}}$, $P(T_K)$ is also power-law like, with an exponent that does not depend on J . This is *not* the power-law regime we refer to in this work). Inset: T_K^{typ} as a function of $1/J$ on a semilog scale. Here we considered $N_a = 1393$, $\mu = -2.2t$, and $N_\phi = 576$.

Kondo coupling J [29]. The dependence of T_K^{typ} on J is shown in the inset of Fig. 2, where we see that we obtain the expected exponential relation [2].

Given the strong energy variations of $\langle \rho_c(\omega) \rangle$, Fig. 1(c), it is then natural to ask whether the form $P(T_K) \propto T_K^{\alpha-1}$ is observed at different locations of the Fermi level μ . We checked that this is indeed the case: in Fig. 3 we show how the exponent α varies with J for several values of μ (to extract the value of α we followed Ref. [42]). The dashed straight lines correspond to the expected behavior at low J (Kondo limit) where we have $\alpha \propto J$ [29, 41].

While the curves α vs J are all qualitatively the same, there are important features associated with the position of μ , and thus the value of $\langle \rho_c(0) \rangle$. Specifically for $\mu = -2.0t$ we enter the NFL region for relatively high values of the Kondo coupling, $J \simeq 2.35t$, and with an average f -level occupation $\langle n_f \rangle \simeq 0.89$ not so close to unity (for all the other values of μ considered $\langle n_f \rangle \simeq 1$). Moreover, for $J = 2.2t$ the thermodynamic properties diverge as a power law with an exponent $1 - \alpha \simeq 0.4$, but if we then vary μ by 10% we get $\alpha \gg 1$ and the system displays FL behavior.

To understand how a power-law distribution of Kondo temperatures emerges in this problem, we closely follow the arguments of Ref. [41]. In the Kondo limit, $\langle n_f \rangle \rightarrow 1$ and $J \rightarrow 0$, it is easy to show that $T_K^\ell = T_K^0 \exp[-\theta_\ell^2]$, where $\theta_\ell^2 = \pi \Delta'_{c\ell}(0)^2 / J \langle \Delta''_{c\ell}(0) \rangle$ and

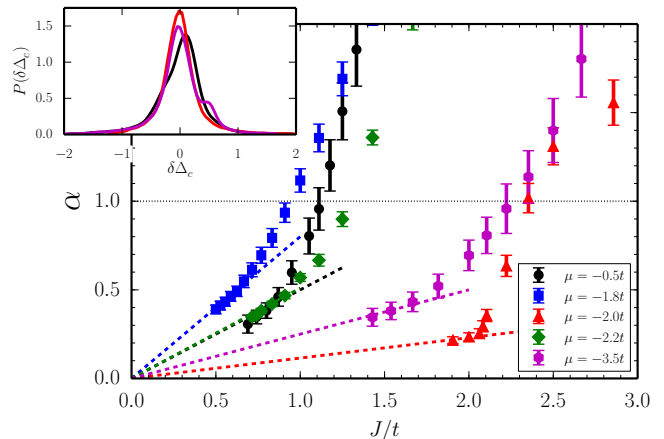


Figure 3: Power-law exponent α as a function of the Kondo coupling J for five different positions of Fermi level μ . The dashed lines are linear fits deep into the Kondo regime where we expect $\alpha \propto J$ to hold (see text). The horizontal dashed line corresponds to $\alpha = 1$ and marks the entrance into the NFL region. At this point we have an average f -level occupation $\langle n_f \rangle = 1 - \langle Z \rangle = 0.970, 0.995, 0.890, 0.995, \text{ and } 0.960$ for $\mu = -0.5t, -1.8t, -2.0t, -2.2t, \text{ and } \mu = -3.5t$, respectively. Here we considered $N_a = 1393$ and $N_\phi = 576$. Inset: distribution of the real part of the local c -electron cavity function fluctuations at the Fermi level $\delta \Delta'_c = \Delta'_c(0) - \langle \Delta'_c(0) \rangle$ for three different values of μ (the color scheme is the same as in the main panel). Here we considered $N_a = 8119$ and $N_\phi = 64$.

$T_K^0 = D \exp[-\pi \langle \Delta''_{c\ell}(0) \rangle / J]$ [29]. Here D is an energy cutoff and $\Delta_{c\ell}(\omega) \equiv \omega - 1/G_{\ell\ell}^c(\omega)$ is the local c -electron cavity function [43] with a single (double) prime denoting its real (imaginary) part. For $\Delta'_{c\ell}(0)$ distributed according to a Gaussian (see the inset of Fig. 3), it then follows immediately that, up to logarithmic corrections, $P(T_K) \propto T_K^{\alpha-1}$, with $\alpha = J \langle \Delta''_{c\ell}(0) \rangle / 2\pi\sigma_c^2$, where σ_c is the variance of $P(\Delta'_{c\ell}(0))$ [29]. Physically, $\Delta'_{c\ell}(0)$ can be interpreted as a renormalized on-site site energy for the c electrons. The simple Gaussian form of $P(\Delta'_{c\ell}(0))$, as in the usual disordered problem [41], suggests an effective self-averaging, in the sense that for local quantities like $\Delta'_{c\ell}(0)$ there seems to be no important distinction between disorder and quasiperiodic order. Nevertheless, we know that this surprising result *cannot* hold for all observables, since, e.g., transport in quasicrystals is known to display “superdiffusive” behavior [11–13].

Finite-size effects and NFL behavior at finite temperatures.— To check the robustness of our scenario against finite-size effects, we performed simulations on approximants of different sizes N_a . For all approximants, we find a minimum Kondo temperature in the sample, T_K^{min} . Below T_K^{min} , FL behavior is then restored within our model (all local moments are screened). From Fig. 2, we learn that the power-law distribution of Kondo temperature $P(T_K) \propto T_K^{\alpha-1}$ emerges for $T_K < T_K^{\text{typ}}$. Taken together, these two observations imply, in principle, that the NFL

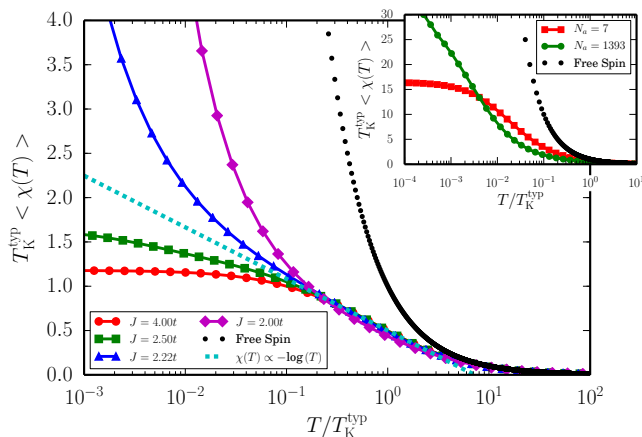


Figure 4: Averaged value of the impurity susceptibility $\langle \chi(T) \rangle$ times the typical value of the Kondo temperature T_K^{typ} as a function of the temperature T normalized by T_K^{typ} for four values of the Kondo coupling J on a semilog scale. For completeness, we show both the free spin and the $\chi \propto -\log(T)$ ($\alpha = 1$) curves. Here we considered $\mu = -2.0t$, $N_a = 1393$, and $N_\phi = 576$. Inset: $T_K^{\text{typ}} \langle \chi(T) \rangle$ as a function of T/T_K^{typ} at $\mu = 2.2t$ and $J = 1.05t$ for two different approximant sizes: $N_a = 7$ and $N_a = 1393$.

range is restricted to the interval $T_K^{\text{min}} < T < T_K^{\text{typ}}$. However, our calculations show that T_K^{min} vanishes as N_a increases while T_K^{typ} remains finite. We thus conclude that the NFL range actually extends down to $T = 0$ in an infinite quasicrystal [29].

To access the finite-temperature behavior of the system and to observe the anticipated NFL behavior, we consider a simple interpolative formula for the local-moment susceptibility, $\chi(T, T_K) = 1/(T + T_K)$, which captures the leading behavior at both low and high- T [2, 29]. We then calculate the magnetic susceptibility of dilute moments as an average of single-impurity contributions, $\langle \chi(T) \rangle = N_a^{-1} \sum_{\ell=1}^{N_a} \chi(T, T_K^\ell)$, with sample results in Fig. 4 [44]. In the region $T \gg T_K^{\text{typ}}$, $\langle \chi(T) \rangle$ shows the expected free-spin form for all values of the Kondo coupling. For $T \ll T_K^{\text{typ}}$, and for $N_a \rightarrow \infty$, we observe two distinct behaviors depending on the value of α . For $\alpha > 1$ we recover the FL behavior at low- T with $\langle \chi(T) \rangle \sim 1/T_K^{\text{typ}}$, whereas for $\alpha < 1$ we obtain $\langle \chi(T) \rangle \propto T^{\alpha-1}$. Moreover, in the crossover region, $T \sim T_K^{\text{typ}}$, we have the surprisingly robust result $\langle \chi(T) \rangle \sim -\log(T)$, regardless of the value of α . This is due to the fact that $P(T_K)$ is essentially flat around T_K^{typ} (Fig. 2). For the smaller approximants, however, T_K^{min} is finite and hence FL behavior must be restored at $T < T_K^{\text{min}}$ for all J . This is explicitly shown in the inset of Fig. 4 where $T_K^{\text{min}} \simeq 10^{-2} T_K^{\text{typ}}$ for $N_a = 7$.

Electronic Griffiths phase and Au₅₁Al₃₄Yb₁₅.—The Kondo-disorder(like) scenario discussed here nicely accounts for power-law divergences in the thermodynamic quantities when dilute Yb local moments are placed

in a metallic quasicrystal. However, the quasicrystal Au₅₁Al₃₄Yb₁₅ forms a dense Kondo lattice, and one may wonder to what extent our scenario is relevant in this context. Based on analogies with disordered Kondo systems (where both the dilute-impurity case and the lattice case produce $P(T_K) \propto T_K^{\alpha-1}$ [19, 41, 45, 46]), we then expect power-law distributions of Kondo temperatures and the corresponding NFL phenomenology for χ and C/T also for the lattice problem. In that case, the NFL region is known as an electronic quantum Griffiths phase and it has by now been observed in several disordered strongly correlated systems [47, 48].

The quasicrystal heavy fermion Au₅₁Al₃₄Yb₁₅ shows NFL behavior with $\chi \sim T^{-0.51}$, $C/T \sim -\log(T)$ [7] or $\chi \sim T^{-0.55}$, $C/T \sim T^{-0.66}$ [8]. Our results, however, predict the same NFL exponent for both χ and C/T , and this difference hampers a definite identification of quantum Griffiths effects [49]. On the other hand, the (Griffiths) power-law divergences are exact only at asymptotically low temperatures, where the regular contribution to the thermodynamic responses may be completely disregarded, and in general the results depend not only on the full form of the $P(T_K)$ curve but also on the particular shape of the scaling functions for the physical observables [29, 44], which may account for differences in the exponent. One such example is the transient $-\log(T)$ divergence in $\langle \chi(T) \rangle$, which is present for all values of the exponent α in the region $T \sim T_K^{\text{typ}}$, Fig. 4.

Interestingly, it was also reported that the temperature dependence of χ and C/T of the quasicrystal Au₅₁Al₃₄Yb₁₅ differs from that of its crystalline approximant. Reference 7 observes no NFL behavior for the approximant, whereas Ref. 8 does observe NFL behavior but with different powers as compared to the quasicrystal. To briefly address this intriguing result, we first notice that the size of the approximant unit cell considered in [7, 8] is small and thus it is reasonable to assume that the experimental situation is similar to the one illustrated in the inset of Fig. 4, where the NFL behavior is bound to be observed only in a relatively narrow range $T_K^{\text{min}} \lesssim T \lesssim T_K^{\text{typ}}$. Moreover, due to the strong energy dependence of $\langle \rho_c(\omega) \rangle$, Fig. 1(c), especially for μ close to a dip (which seems to be case for Au₅₁Al₃₄Yb₁₅ [50]), tiny variations in parameters, such as the band filling or Kondo coupling, may drive the system to or from a NFL behavior. Therefore, care should be taken when drawing any conclusions from this distinct behavior.

Conclusions.—Motivated by the recently observed NFL behavior in the heavy-fermion quasicrystal Au₅₁Al₃₄Yb₁₅, we investigated the single-impurity Kondo effect in the octagonal (2D) and icosahedral (3D) tilings. We found a power-law distribution of Kondo temperatures $P(T_K) \propto T_K^{\alpha-1}$ and corresponding NFL behavior, in a surprising similarity to disordered metals. Therefore, a quasicrystalline conduction band provides a natural route to the emergence of a robust NFL behav-

ior without the tuning of external parameters as doping, pressure, or external field. For the Kondo quasicrystalline lattice problem, we expect, based on the analogy to disordered systems [17], a similar NFL behavior to be observed. In addition, it would be interesting to investigate the feedback effect of the local moments, in particular moments with $T_K < T$, on the transport properties of the quasicrystalline conduction electrons and the effects of intersite spin correlations [51].

We gratefully acknowledge help from M. Mihalkovic with approximants of the 3D icosahedral tiling. A.J. thanks P. Coleman for useful discussions on the quasiperiodic heavy fermion $\text{Au}_{51}\text{Al}_{34}\text{Yb}_{15}$. E.C.A. was supported by FAPESP (Brazil) Grant No. 2013/00681-8. E.M. was supported by CNPq (Brazil) Grants No. 304311/2010-3 and No. 590093/2011-8. M.V. was supported by the Helmholtz association through VI-521 and by the DFG Grants No. GRK 1621 and No. SFB 1143. V.D. was supported by the NSF Grants No. DMR-1005751 and No. DMR-1410132.

-
- [1] N. W. Ashcroft and N. D. Mermin, *Solid State Physics* (Thomson Learning, 1976), 1st ed.
- [2] A. C. Hewson, *The Kondo Problem to Heavy Fermions* (Cambridge University Press, Cambridge, 1993), 1st ed.
- [3] G. R. Stewart, *Rev. Mod. Phys.* **73**, 797 (2001).
- [4] M. Brian Maple, R. E. Baumbach, N. P. Butch, J. J. Hamlin, and M. Janoschek, *J. Low Temp. Phys.* **161**, 4 (2010).
- [5] P. Coleman, C. Pépin, Q. Si, and R. Ramazashvili, *J. Phys. Condens. Matter* **13**, R723 (2001).
- [6] H. v. Löhneysen, A. Rosch, M. Vojta, and P. Wölfle, *Rev. Mod. Phys.* **79**, 1015 (2007).
- [7] K. Deguchi, S. Matsukawa, N. K. Sato, T. Hattori, K. Ishida, H. Takakura, and T. Ishimasa, *Nat. Mater.* **11**, 1013 (2012).
- [8] T. Watanuki, S. Kashimoto, D. Kawana, T. Yamazaki, A. Machida, Y. Tanaka, and T. J. Sato, *Phys. Rev. B* **86**, 094201 (2012).
- [9] M. Kohmoto, B. Sutherland, and C. Tang, *Phys. Rev. B* **35**, 1020 (1987).
- [10] H. Tsunetsugu, T. Fujiwara, K. Ueda, and T. Tokihiro, *Phys. Rev. B* **43**, 8879 (1991).
- [11] H. Q. Yuan, U. Grimm, P. Repetowicz, and M. Schreiber, *Phys. Rev. B* **62**, 15569 (2000).
- [12] U. Grimm and M. Schreiber, in *Quasicrystals - Structure and Physical Properties*, edited by H.-R. Trebin (Wiley-VCH, Weinheim, 2003), pp. 210–235.
- [13] A. Jagannathan and F. Piéchon, *Philos. Mag.* **87**, 2389 (2007).
- [14] G. T. de Laissardière and D. Mayou, *C. R. Physique* **15**, 70 (2014).
- [15] S. Watanabe and K. Miyake, *J. Phys. Soc. Jpn.* **82**, 083704 (2013).
- [16] V. R. Shaginyan, A. Z. Msezane, K. G. Popov, G. S. Japaridze, and V. A. Khodel, *Phys. Rev. B* **87**, 245122 (2013).
- [17] E. Miranda and V. Dobrosavljević, *Rep. Prog. Phys.* **68**, 2337 (2005).
- [18] V. Dobrosavljević, T. R. Kirkpatrick, and B. G. Kotliar, *Phys. Rev. Lett.* **69**, 1113 (1992).
- [19] E. Miranda, V. Dobrosavljević, and G. Kotliar, *J. Phys. Cond. Mat* **8**, 9871 (1996).
- [20] P. S. Cornaglia, D. R. Grempel, and C. A. Balseiro, *Phys. Rev. Lett.* **96**, 117209 (2006).
- [21] S. Kettemann, E. R. Mucciolo, and I. Varga, *Phys. Rev. Lett.* **103**, 126401 (2009).
- [22] S. Kettemann, E. R. Mucciolo, I. Varga, and K. Slevin, *Phys. Rev. B* **85**, 115112 (2012).
- [23] V. G. Miranda, L. G. G. V. Dias da Silva, and C. H. Lewenkopf, *Phys. Rev. B* **90**, 201101 (2014).
- [24] D. Shechtman, I. Blech, D. Gratias, and J. W. Cahn, *Phys. Rev. Lett.* **53**, 1951 (1984).
- [25] A. P. Smith and N. W. Ashcroft, *Phys. Rev. Lett.* **59**, 1365 (1987).
- [26] E. S. Zijlstra and T. Janssen, *Europhys. Lett.* **52**, 578 (2000).
- [27] A. Richardella, P. Roushan, S. Mack, B. Zhou, D. A. Huse, D. D. Awschalom, and A. Yazdani, *Science* **327**, 665 (2010).
- [28] A. Rodriguez, L. J. Vasquez, K. Slevin, and R. A. Römer, *Phys. Rev. Lett.* **105**, 046403 (2010).
- [29] See Supplemental Material, which includes Refs. [52–61], for a detailed description of our numerical approach, further information on the octagonal tiling, the derivation of an asymptotic expression for $P(T_K)$, and results for the 3D icosahedral tiling.
- [30] As argued in J. Luck and D. Petritis, *J. Stat. Phys.* **42**, 289 (1986), the lower critical dimension for the existence of critical states in quasicrystals is $1D$. In this sense, there should not be significant qualitative differences between electronic quasicrystalline states in $2D$ and $3D$.
- [31] J. E. S. Socolar, *Phys. Rev. B* **39**, 10519 (1989).
- [32] D. Levine and P. J. Steinhardt, *The Physics of Quasicrystals* (World Scientific, Singapore, 1987).
- [33] M. Duneau, *J. Phys. A: Math. Gen.* **22**, 4549 (1989).
- [34] V. G. Benza and C. Sire, *Phys. Rev. B* **44**, 10343 (1991).
- [35] C. Gros, *Phys. Rev. B* **53**, 6865 (1996).
- [36] T. Rieth and M. Schreiber, *Phys. Rev. B* **51**, 15827 (1995).
- [37] N. Read and D. M. Newns, *J. Phys. C* **16**, 3273 (1983).
- [38] N. Read and D. M. Newns, *J. Phys. C* **16**, L1055 (1983).
- [39] P. Coleman, *Phys. Rev. B* **29**, 3035 (1984).
- [40] Because the $U \rightarrow \infty$ Anderson impurity model is particle-hole asymmetric, this definition of T_K is, in general, close but not equal to the onset temperature of a non-trivial solution ($Z_\ell \neq 0$, $\tilde{\epsilon}_{f\ell} \neq E_f$) of the saddle-point equations.
- [41] D. Tanasković, E. Miranda, and V. Dobrosavljević, *Phys. Rev. B* **70**, 205108 (2004).
- [42] A. Clauset, C. R. Shalizi, and M. E. J. Newman, *SIAM Review* **51**, 661 (2009).
- [43] V. Dobrosavljević and G. Kotliar, *Phil. Trans. R. Soc. Lond. A*, **356**, 57 (1998).
- [44] Using this interpolative formula it is easy to see that $\langle \chi(T) \rangle = \int dT_K P(T_K) / (T + T_K) = \chi_r + \chi_s$. χ_r is a regular contribution whereas $\chi_s \propto T^{\alpha-1}$ gives rise to NFL behavior for $\alpha < 1$ as $T \rightarrow 0$.
- [45] E. Miranda and V. Dobrosavljević, *Phys. Rev. Lett.* **86**, 264 (2001).
- [46] R. K. Kaul and M. Vojta, *Phys. Rev. B* **75**, 132407 (2007).

- [47] E. C. Andrade, E. Miranda, and V. Dobrosavljević, Phys. Rev. Lett. **102**, 206403 (2009).
- [48] M. C. O. Aguiar and V. Dobrosavljević, Phys. Rev. Lett. **110**, 066401 (2013).
- [49] T. Vojta, J. Low Temp. Phys. **161**, 299 (2010).
- [50] S. Jazbec, S. Vrtnik, Z. Jagličić, S. Kashimoto, J. Ivkov, P. Popčević, A. Smontara, H. J. Kim, J. G. Kim, and J. Dolinšek, J. Alloys Compd. **586**, 343 (2014).
- [51] D. Tanasković, V. Dobrosavljević, and E. Miranda, Phys. Rev. Lett. **95**, 167204 (2005).
- [52] A. Chhabra and R. V. Jensen, Phys. Rev. Lett. **62**, 1327 (1989).
- [53] A. D. Mirlin, Phys. Rep. **326**, 259 (2000).
- [54] G. Schubert, J. Schleede, K. Byczuk, H. Fehske, and D. Vollhardt, Phys. Rev. B **81**, 155106 (2010).
- [55] F. F. Assaad, in *Quantum Simulations of Complex Many-Body Systems: From Theory to Algorithms*, edited by J. Grotendorst, D. Marx, and A. Muramatsu ((John von Neumann Institute for Computing (NIC), 2002).
- [56] William H. Press *et al.*, *Numerical Recipes: The Art of Scientific Computing* (Cambridge University Press, 2007), 3rd ed.
- [57] A. Jagannathan, Phys. Rev. B **61**, R834 (2000).
- [58] D. S. Fisher, Phys. Rev. B **51**, 6411 (1995).
- [59] T. Vojta, J. Phys. A: Math. Gen. **39**, R143 (2006).
- [60] P. W. Anderson, Phys. Rev. **109**, 1492 (1958).
- [61] E. Abrahams, P. W. Anderson, D. C. Licciardello, and T. V. Ramakrishnan, Phys. Rev. Lett. **42**, 673 (1979).

Supplementary information for:

“Non-Fermi-liquid behavior in metallic quasicrystals with local magnetic moments”

Eric C. Andrade,¹ Anuradha Jagannathan,² Eduardo Miranda,³ Matthias Vojta,⁴ and Vladimir Dobrosavljević⁵¹*Instituto de Física Teórica, Universidade Estadual Paulista,**Rua Dr. Bento Teobaldo Ferraz, 271 - Bl. II, 01140-070, São Paulo, SP, Brazil*²*Laboratoire de Physique des Solides, CNRS-UMR 8502, Université Paris-Sud, 91405 Orsay, France*³*Instituto de Física Gleb Wataghin, Unicamp, Rua Sérgio Buarque de Holanda, 777, CEP 13083-859 Campinas, SP, Brazil*⁴*Institut für Theoretische Physik, Technische Universität Dresden, 01062 Dresden, Germany*⁵*Department of Physics and National High Magnetic Field Laboratory, Florida State University, Tallahassee, FL 32306*

(Dated: October 23, 2018)

I. ELECTRONIC WAVEFUNCTIONS IN THE OCTAGONAL TILING

Based on the results for one-dimensional quasicrystals,¹ we expect the resulting wavefunctions in quasiperiodic tight-binding models to be different both from the exponentially localized wavefunctions found in Anderson insulators as well from Bloch states found in a crystal. Such wavefunctions are the so-called *critical* wavefunctions. In real space, this means very large fluctuations of the wavefunction amplitude from site to site but with similar amplitudes on sites of similar local environment (the amplitude distribution is thus determined by the deterministic scale invariant geometry).

To probe the real space profile of the wavefunctions, we compute the inverse participation ratio

$$P_\nu^{-1} = \sum_i |\psi_\nu^c(i)|^4, \quad (\text{S1})$$

where ψ_ν^c is an eigenstate of \mathcal{H}_c (defined in Eq. [1] of the main text) with energy E_ν^c . The scaling of P_ν^{-1} with the system size is related to the spatial structure of the electronic states. If we write $P_\nu^{-1} \propto N_a^{-\beta}$, then $\beta = 1$ for extended and $\beta = 0$ for exponentially localized states. In a quasicrystal, because of the critical nature of the wavefunctions, we expect that $0 \leq \beta \leq 1$. It is important to point out that the converse it is not true. For instance, $\beta \approx 1$ does not necessarily imply an extended state. To establish such result, we need to study the scaling of the higher moments of the wavefunction distribution because the exponents that describe the scaling of these moments with N_a are not just multiples of each other – a property of multifractality.^{2–4} As mentioned above, this resulting multifractal character of wavefunctions is a consequence of the invariance of quasicrystals under scale transformations, a feature called inflation-deflation symmetry.⁵

In Fig. S1 we calculate P_ν^{-1} at different positions in the band (but away from the band center) and obtain $\beta \approx 0.90$, which is close but smaller than one and consistent with a preponderance of multifractal eigenstates. Remarkably, this is similar to the value of β reported for the Penrose tiling.⁶

Another useful quantity that probes the nature of the

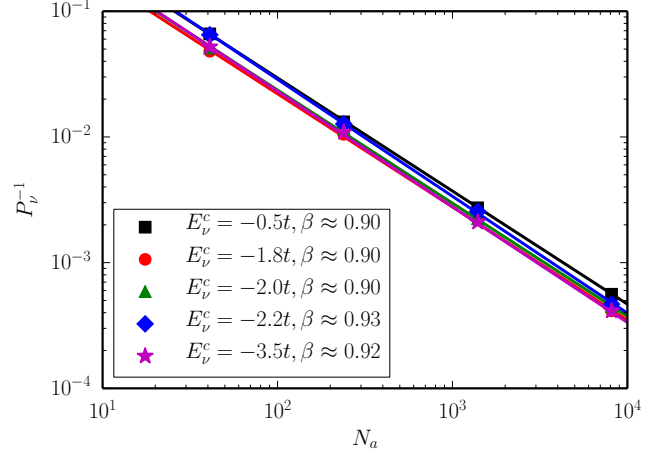


Figure S1: Octagonal tiling. Inverse participation ratio P_ν^{-1} as a function of the approximant size N_a for different values of the eigenenergies E_ν^c on a log-log scale. We considered four approximant sizes $N_a = 41, 239, 1393, 8119$. The solid lines are power-law fits: $P_\nu^{-1} \propto N_a^{-\beta}$.

wavefunction is the local density of states (LDOS)

$$\rho_i^c(\omega) = \overline{\sum_\nu |\psi_\nu^c(i)|^2 \delta(\omega - E_\nu^c)}, \quad (\text{S2})$$

where the overline denotes average over boundary conditions. The distribution of the logarithm of $\rho_i^c(\omega)$ is presented in Fig. S2. As we can see, the curves are all qualitatively the same, indicating that the spatial fluctuations of ρ_i^c are, to a good extent, energy-independent and well described by a log-normal distribution (see the inset). Specifically, the width of the distribution does not vary much with the energy, except for $\omega = -2.0t$ where there is a slightly larger tendency to have $\rho_i^c(\omega)$ smaller than its typical value.

Generally, a log-normal distribution of LDOS is expected to occur in an Anderson insulator,⁷ but it is also known that a log-normal also nicely describes the distribution of LDOS of disordered metals.⁸ Therefore, a careful finite-size scaling study is required to establish the precise nature of the wavefunction based on $P(\rho)$.⁸ We leave this more detailed investigation for a future work.

To conclude the discussion on the octagonal tiling,

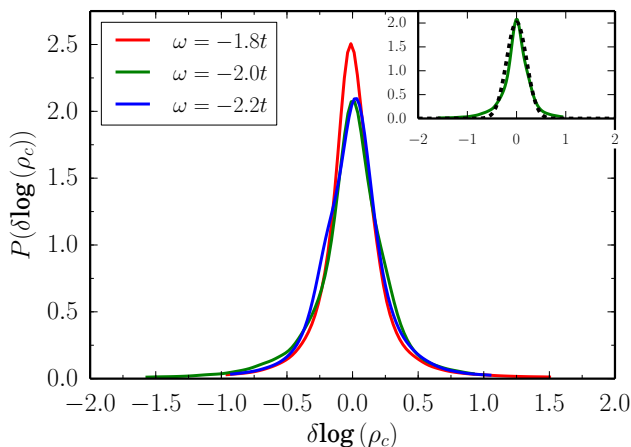


Figure S2: Octagonal tiling. Distribution of $\delta \log(\rho_c) = \log(\rho_c) - \langle \log(\rho_c) \rangle$ at three different values of the energy ω . Inset: The full curve correspond to $P(\delta \log(\rho_c))$ at $\omega = -2.0t$ and the dashed curve is a Gaussian fit to it. Here we considered the $N_a = 8119$ approximant with $N_\phi = 64$.

we briefly mention our implementation of averaging over twisted boundary conditions (TBC).^{9,10} This step was instrumental in obtaining reliable results since it provides a controlled way to eliminate finite-size effects associated with spectral discreteness (we will come back to the role of finite-size effects later). The average over TBC is completely equivalent to a periodic repetition of the N_a -site approximant in both directions using N_ϕ copies, hence the effective total linear system size is increased to $\sqrt{N_a N_\phi}$.

II. SLAVE BOSONS MEAN-FIELD EQUATIONS AND THE KONDO LIMIT

Minimizing the slave boson (SB) mean-field free energy, Eq. [2] in the main text, with respect to $\tilde{\varepsilon}_\ell$ and Z_ℓ we obtain the corresponding self-consistency equations

$$\begin{aligned} \frac{2}{\pi} \int_{-\infty}^{+\infty} f(\omega) \text{Im} \left[\tilde{G}_\ell^f(\omega) \right] d\omega + Z_\ell - 1 &= 0, \quad (\text{S3}) \\ \frac{2}{\pi} \int_{-\infty}^{+\infty} f(\omega) \text{Im} \left[\tilde{G}_\ell^f(\omega) \Delta_{f\ell}(\omega) \right] d\omega + \\ \tilde{\varepsilon}_{f\ell} - E_f &= 0. \quad (\text{S4}) \end{aligned}$$

In general, we solve these mean-field equations numerically at $T = 0$. They are algebraic non-linear equations on the parameters Z_ℓ and $\tilde{\varepsilon}_{f\ell}$, which we solve using a globally convergent implementation of the Newton-Raphson algorithm.¹¹ The integral over frequencies is performed using the Romberg method.¹¹

If we now move to the Kondo limit, where both $Z_\ell, \tilde{\varepsilon}_{f\ell} \rightarrow 0$, we are able to solve Eqs. (S3) and (S4) analytically. In this limit, we ignore the frequency dependence of the hybridization function, $\Delta_{f\ell}(\omega) \simeq \Delta'_{f\ell}(0) +$

$i\Delta''_{f\ell}(0)$, and assume that the integrals are dominated by their values at the Fermi level. From Eq. (S3) we obtain

$$\tilde{\varepsilon}_f + Z_\ell \Delta'_{f\ell}(0) \simeq 0. \quad (\text{S5})$$

which reflects the well-known fact that in the Kondo limit the position of the Kondo peak, $\tilde{\varepsilon}_f + Z_\ell \Delta'_{f\ell}(0)$, moves to the Fermi level.

From Eq. (S4) we can now calculate the Kondo temperature (recall our definition $T_K^\ell \equiv Z_\ell \Delta''_{f\ell}(0)$)

$$T_K^\ell = D \exp \left[-\frac{\pi}{2} \frac{\Delta'_{f\ell}(0) + |E_f|}{\Delta''_{f\ell}(0)} \right], \quad (\text{S6})$$

where D is a high-energy cutoff of the integral of the order of the bandwidth. We recover the usual Kondo expression, $T_K^\ell = D \exp[-1/J\rho_\ell^c(0)]$, in the case of particle-hole symmetry, $\Delta'_{f\ell}(0) = 0$, with $\Delta''_{f\ell}(0) = \pi V^2 \rho_\ell^c(0)$ and $J = 2V^2/|E_f|$.

III. ASYMPTOTIC EXPRESSION FOR $P(T_K)$

Each site of the tiling has a different local c -electron cavity function $\Delta_{c\ell}(\omega)$, reflecting the fact that the effective potential that one electron sees as it goes through the lattice changes from site to site. If we go one step further, we may consider its real part at the Fermi level, $\Delta'_{c\ell}(0)$, as a renormalized on-site site energy for the c -electrons. According to the arguments presented in Ref. 12 for the case of weakly disordered Kondo systems, a power-law distribution for the Kondo temperature can be easily obtained provided that the fluctuations of $\Delta'_{c\ell}(0)$, $\delta\Delta'_c \equiv \Delta'_c(0) - \langle \Delta'_c(0) \rangle$, follow a Gaussian distribution (see the inset of Fig. 3 of the main text). In disordered systems, the fluctuations of the local c -electron cavity function at a given site i result from Friedel oscillations of the electronic wavefunctions induced by other impurities which may lie at a relatively long distance from i . Furthermore, at weak disorder, $\delta\Delta'_{c\ell}$ takes the form of a linear superposition of contributions from single impurity scatterers, and thus of a sum of independent random numbers, for which we expect the central limit theorem to hold. From our numerical results, we then reason that a similar mechanism takes place in quasicrystals. This somewhat surprising resemblance between a quasicrystal and weakly disordered systems, rather than systems at the metal-insulator transition, is also present in different physical quantities, e.g. the level-spacing distribution.^{5,6,13} It indicates that a quasicrystal in higher dimensions may show a more conventional behavior in local quantities despite its multifractal eigenstates.

It is now a straightforward exercise to obtain the asymptotic expression $P(T_K) \sim T_K^{\alpha-1}$ following Ref. 12. We start by relating the f -level hybridization function $\Delta_{f\ell}$ with the local c -electron cavity function $\Delta_{c\ell}$ at the

impurity site ℓ

$$\Delta'_{f\ell}(\omega) = \frac{V^2(\omega - \Delta'_{c\ell}(\omega))}{(\omega - \Delta'_{c\ell}(\omega))^2 + (\Delta''_{c\ell}(\omega))^2}, \quad (\text{S7})$$

$$\Delta''_{f\ell}(\omega) = \frac{V^2\Delta''_{c\ell}(\omega)}{(\omega - \Delta'_{c\ell}(\omega))^2 + (\Delta''_{c\ell}(\omega))^2}, \quad (\text{S8})$$

where, as usual, single (double) primes denote the real (imaginary) part. The next step is to take the Kondo limit making use of Eq. (S6). As the last assumption, we disregard fluctuation in the imaginary part of $\Delta_{c\ell}(0)$, so we replace $\Delta''_{c\ell}(0)$ by its average value $\langle\Delta''_c(0)\rangle$. Using Eqs. (S7) and (S8) we then obtain

$$T_K^\ell = T_K^0 \exp\left[-\pi \frac{(\Delta'_{c\ell}(0))^2}{J\langle\Delta''_c(0)\rangle}\right], \quad (\text{S9})$$

where $T_K^0 \equiv D \exp[-\pi\langle\Delta''_c(0)\rangle/J]$. Inverting Eq. (S9) we may write

$$\delta\Delta'_{c\ell} \simeq \ln^{1/2}\left[\frac{T_K^0}{T_K^\ell}\right]^\lambda, \quad (\text{S10})$$

with $\lambda = J\langle\Delta''_c(0)\rangle/\pi$ and we also considered the fact that for $T_K^\ell \ll T_K^0$ we may drop the the term $\langle\Delta'_{c\ell}(0)\rangle$. Since we assume that $P(\delta\Delta'_c)$ is a simple Gaussian with variance σ_c , a direct change of variables gives, up to a negligible logarithmic correction,

$$P(T_K) \propto T_K^{\alpha-1}, \quad (\text{S11})$$

with

$$\alpha = \frac{J\langle\Delta''_c(0)\rangle}{2\pi\sigma_c^2} \sim J\langle\rho_c(0)\rangle. \quad (\text{S12})$$

So we see that α varies linearly with J with a slope proportional to $\langle\rho_c(0)\rangle$.

To check the plausibility of our assumptions, we produced a scatter plot of the numerically calculated T_K^ℓ versus the exponent of the Kondo limit formulas for T_K^ℓ in Eqs. (S6) and (S9), Fig. S3. There, we see that all the points (one for each site in the quasicrystal approximant) follow a straight line, specially as T_K^ℓ decreases, clearly indicating a strong correlation between the full numerics and the asymptotic expressions for the T_K^ℓ . Additional scatter around this straight line simply reflects departures from Eqs. (S6) and (S9), i.e. a situation where the value T_K^ℓ depends not only on $\Delta_{f\ell}$ at the Fermi level, but on the entire spectral function. Moreover, as T_K^ℓ decreases the curves obtained from Eqs. (S6) and (S9) become more and more similar showing that the fluctuations in $\Delta'_{c\ell}(0)$ are indeed the dominant ones.

The power-law distribution of Kondo temperatures describes only the low- T_K tail of the full distribution $P(T_K)$ and we then expect that our asymptotic expressions in Eqs. (S11) and (S12) to work better and better as α

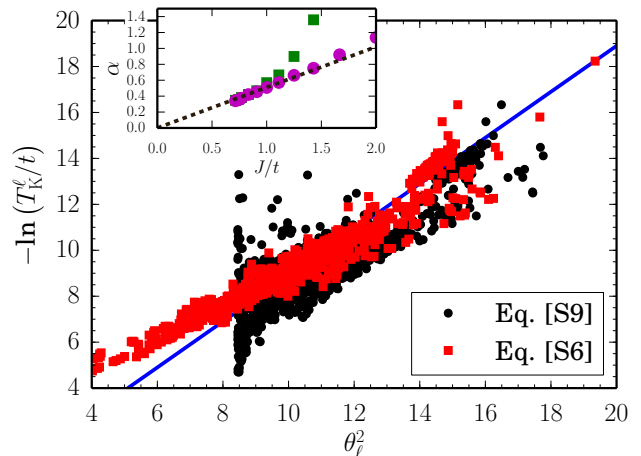


Figure S3: Octagonal tiling. Scatter plot of the numerically calculated $-\ln(T_K^\ell)$ as a function of the exponent θ_ℓ^2 with $\theta_\ell^2 = \pi(\Delta'_{f\ell}(0) + |E_f|)/2\Delta''_{f\ell}(0)$ (Eq. (S6)) or $\theta_\ell^2 = \pi(\Delta'_{c\ell}(0))^2/J\langle\Delta''_c(0)\rangle$ (Eq. (S9)). Each point correspond to a given site in the approximant and the straight line has a unity slope. Here, we considered the $N_a = 1393$ approximant, $J = 0.77t$, and $\mu = -2.2t$. Inset: Power-law exponent α for $\mu = -2.2t$ as a function of the Kondo coupling J . The squares correspond to the exponent extracted from the numerical data as in Fig. 3 of the main text. The circles correspond to the exponent extracted from a distribution of T_K generated according to Eq. (S6). The dashed line is the asymptotic expression for α in Eq. (S12). The error bars for α are smaller than the symbol sizes.

(or J) diminishes. To check this, we compare the exponent α from our numerical data with: (i) the exponent extracted from a distribution of T_K generated according to Eq. (S6); and (ii) the asymptotic expression for α in Eq. (S12). In the inset of Fig. S3 we show that all three values of α nicely match for $J \lesssim 1t$.

IV. SINGULAR KONDO TEMPERATURE DISTRIBUTION AND NFL BEHAVIOR

As we discussed in the main text, the region in which $\alpha < 1$ corresponds to NFL behavior at low- T . To establish this link, we combine our $T = 0$ solution of the mean field equations (S3) and (S4) with the well-known scaling relations for the Kondo impurity problem.¹⁴ Essentially, we use the fact that the Kondo problem has a single energy scale, the Kondo temperature T_K , and that the observables can be written as universal functions of T/T_K .

For instance, for the local-moment susceptibility we have

$$\chi(T, T_K) \propto \frac{1}{T_K} f\left(\frac{T}{T_K}\right), \quad (\text{S13})$$

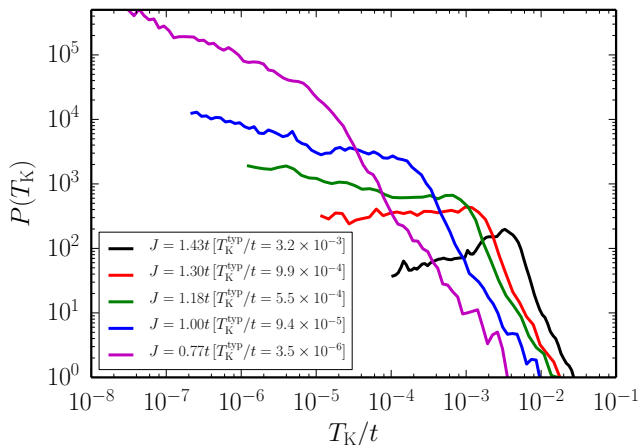


Figure S4: Octagonal tiling. Distribution of the local Kondo temperatures $P(T_K)$ as a function of T_K on a log-log scale for several values of the Kondo coupling J . J increases from the top to the bottom curve. We see that for $T_K \lesssim T_K^{\text{typ}}$ this distribution acquires a power-law form $P(T_K) \sim T_K^{\alpha-1}$. The power-law exponent α continuously varies with the coupling J and for $\alpha < 1$ we have a singular distribution (notice that for $T_K \gtrsim T_K^{\text{typ}}$, $P(T_K)$ is also power-law like, with a power that does not depend on J . This is *not* the power-law regime we refer to in this work). Here we considered $N_a = 1393$, $\mu = -2.2t$, and $N_\phi = 576$.

with the asymptotic forms of $f(x)$ given by¹⁴

$$f(x) = \begin{cases} a - bx^2 & x \ll 1 \\ (c/x)(1 - 1/\ln x) & x \gg 1 \end{cases}, \quad (\text{S14})$$

where a , b , and c are universal numbers. The average value of the susceptibility is then given by

$$\begin{aligned} \langle \chi(T) \rangle &= \int dT_K P(T_K) \chi(T, T_K) \\ &= \chi_r + \underbrace{\int_0^{T_K^{\text{max}}} dT_K T_K^{\alpha-1} \frac{1}{T_K} f\left(\frac{T}{T_K}\right)}_{\propto T^{\alpha-1}} \end{aligned} \quad (\text{S15})$$

Here, $T_K^{\text{max}} \sim T_K^{\text{typ}}$ is a cutoff below which the power-law form of $P(T_K)$ holds and we see that $\langle \chi(T) \rangle$ contains a regular part χ_r and a potentially singular contribution $\chi_s \propto T^{\alpha-1}$. For $\alpha < 1$ and at low- T , we may then disregard χ_r to obtain the anticipated NFL power-law divergence $\langle \chi(T) \rangle \propto T^{\alpha-1}$. The impurity specific heat divided by the temperature has a similar behavior and, accordingly, we get $\langle C/T \rangle \propto T^{\alpha-1}$.

Given that the SB mean-field approach can be applied at finite- T (albeit resulting in an unphysical finite-temperature transition) it is then natural to ask ourselves whether it is legitimate to calculate $P(T_K)$ at $T = 0$, and follow the procedure described above, rather than solving the SB equations at finite- T to explicitly calculate $\chi(T)$ and $\gamma(T)$. From our experience, the general conclusion is that the leading low- T power-law behavior of χ

or C/T is not affected by these additional effects. Higher- T behavior will of course be affected but as long as we are interested in leading low- T asymptotics (the value of the power), the current procedure is well-defined, simply because the distributions $P(T_K)$ are very broad. Similar questions have been raised in the more general context of Quantum Griffiths Phases and the Infinite-Randomness Fixed Point Behavior.¹⁵ There again one arrives at a similar conclusion: the $T = 0$ distribution of energy dominates even finite- T behavior.¹⁶⁻¹⁸

In the same spirit, we may extend the above discussion to also calculate observables other than thermodynamical. An interesting quantity to look at is the nuclear spin-lattice relaxation rate divided by temperature $1/(T_1T)$. In our Griffiths scenario, we expect that $1/(T_1T) \sim T^{\alpha-2} \sim \chi/T$.¹⁸⁻²⁰ Nevertheless, the experiment finds that $1/(T_1T) \sim \chi$.²¹ We point out, however, that this discrepancy is not, at this point, particularly conclusive, since the curves for $1/(T_1T)$ in Ref. 21 were obtained only for $T > 1K$, whereas the NFL behavior is more pronounced for $T < 1K$. It would be nice to see how $1/(T_1T)$ behaves at low temperatures, where it will most certainly provide more conclusive hints as for the nature of quasicrystalline electronic environment. Another interesting quantity to investigate is the resistivity.^{19,20} However, unlike thermodynamic responses, for which we expect the single impurity behavior to survive in the dense lattice limit (as is the case of $\text{Au}_{51}\text{Al}_{34}\text{Yb}_{15}$), we know that for transport the situation will be different as coherence between the impurities emerges and thus we cannot, at this point, compare our predictions to the experiments. Furthermore, we expect this to be a non-trivial problem, because even in the absence of correlations, transport in quasicrystals is known to display an unusual “super-diffusive” behavior.^{5,6,22}

V. SIZE DEPENDENCE OF $P(T_K)$

In this work, we consider different values of N_a in order to establish what happens for a true quasicrystal ($N_a \rightarrow \infty$). As we mention in the main text, for all approximant sizes N_a we find a minimum Kondo temperature in the sample, T_K^{min} . For the smaller approximants, the six local environments of the octagonal tiling (Fig. 1(b) of the main text) appear in a modest number of different arrangements. In other words, their extended environment, including next-nearest and further neighbors is limited. This leads not only to an appreciable T_K^{min} but also to few distinct values of T_K . As we increase the approximant size, these local environments appear in further unique configurations leading to more and more values of T_K in the sample. Therefore, we expect the statistics of T_K to improve with N_a , which can be clearly seen in Fig. S5, where, for instance, the peak around $T_K^{\text{typ}} \sim 10^{-3}t$ (which hardly varies with N_a) becomes ever more well defined as the system size increases. The most important, however, is the ubiquitous presence of

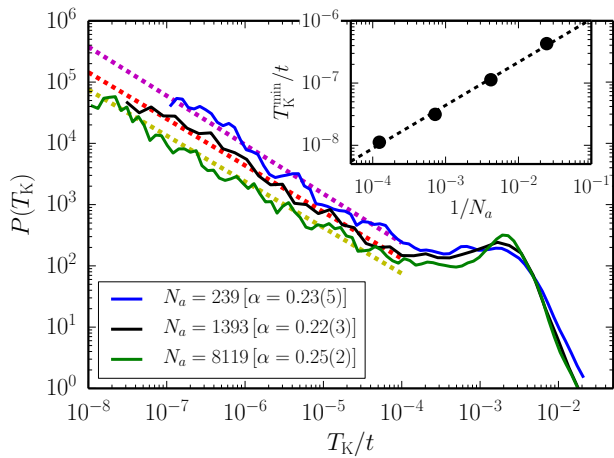


Figure S5: Octagonal tiling. Distribution of Kondo temperatures $P(T_K^{\max})$ as a function of T_K for $\mu = -2.0t$ and $J = 2.0t$ and three different approximant sizes N_a . The dashed lines are a power-law fits with $T_K^{\max} = 10^{-4}t$ with the corresponding exponents α shown in the caption. Inset: Minimum value of the Kondo temperature T_K^{\min} a function of the inverse approximant size. The dashed line is a power-law fit with $T_K^{\min} \propto N_a^{-0.69}$.

the power-law tail at low- T_K in Fig. S5 for all three approximant sizes with the same exponent (within error bars). Moreover, it is also clear from Fig. S5 that T_K^{\min} is suppressed with increasing N_a . Indeed, in the inset of Fig. S5 we find a power-law dependence of T_K^{\min} on N_a : $T_K^{\min} \propto N_a^{-0.69}$. Such power-law finite-size scaling (with a nontrivial power) is precisely what one expects in a critical state (in a conventional metal, for instance, one would expect power-law finite-size scaling—as it is gapless—but with integer powers).

Within our model, FL behavior is restored below T_K^{\min} as all local moments are then screened. Since the power-law distribution of Kondo temperature $P(T_K) \propto T_K^{\alpha-1}$ emerges for $T_K < T_K^{\text{typ}}$, we could expect, in principle, the NFL range to be constrained to the interval $T_K^{\min} < T < T_K^{\text{typ}}$. However, as Fig. S5 shows, T_K^{\min} vanishes as N_a increases while T_K^{typ} remains finite. We thus conclude that the NFL range actually extends down to $T = 0$ in a real quasicrystal. Therefore, our results suggest that it is not their local structure, but the lack of long-distance periodicity which induces robust NFL behavior in quasicrystals.

VI. NUMERICAL CALCULATION OF THE POWER-LAW EXPONENT α

Here we address how we calculate the power-law exponent α governing the low- T_K part of the distribution of Kondo temperatures. The straightforward way is to plot $P(T_K)$ on a log-log scale and then extract $(\alpha - 1)$ as the slope of the resulting straight line. While well defined, this procedure extracts α not from the data itself, but

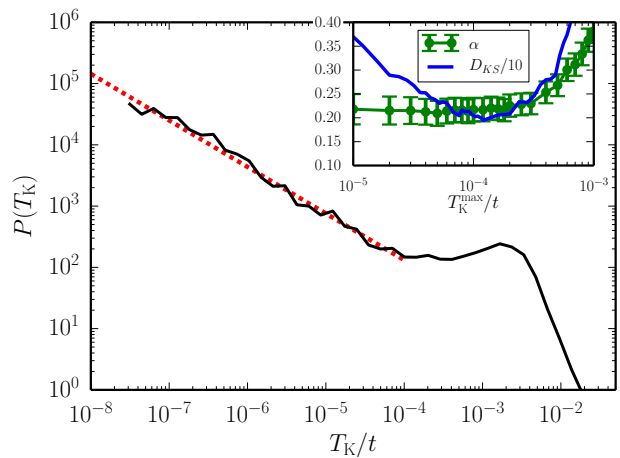


Figure S6: Octagonal tiling. Distribution of Kondo temperatures $P(T_K)$ as a function of T_K for $\mu = -2.0t$ and $J = 2.0t$. The dashed line shows a power-law fit with $\alpha = -0.24$ and $T_K^{\max} = 10^{-4}t$. Inset: The circles shows the value of α , as calculated from Eq. (S16), whereas the full line show the Kolmogorov-Smirnov (KS) test as a function of T_K^{\max} . Here we considered the $N_a = 1393$ approximant.

from a given histogram. We complement the latter procedure calculating α directly from the data as explained in Ref. 23.

Given a data set containing n observations $T_K \leq T_K^{\max}$, where T_K^{\max} is the largest value of the energy scale for which the power-law distribution holds, the value of α that is most likely to have generated our data is given by

$$\alpha = \frac{n}{\sum_{i=1}^n \ln [T_K^{\max}/T_K^i]}, \quad (\text{S16})$$

with an error

$$\sigma_\alpha = \alpha/\sqrt{n}. \quad (\text{S17})$$

In practice, however, the greatest source of error comes from not choosing an optimal value for T_K^{\max} , which we dub $T_K^{\max*}$. We then implement two procedures to estimate $T_K^{\max*}$.²³ In the first one, we plot $\alpha \times T_K^{\max}$ and define $T_K^{\max*}$ as the point around which α is stable as we vary T_K^{\max} . The second procedure follows the spirit of a chi-square test. The idea is to investigate how well our data is fitted by a power-law distribution. Since we are now dealing with distributions, we implement the so-called Kolmogorov-Smirnov (KS) test.¹¹ The KS statistics D_{KS} is defined as the maximum value of the absolute difference between the two *cumulative* distribution functions. We then attempt to minimize D_{KS} as a function of T_K^{\max} .

In Fig. S6 we illustrate the discussion above. In the main panel we show $P(T_K)$ on a log-log plot accompanied by a power-law fit to its low- T_K tail. In the fit displayed here, we considered $T_K^{\max} = 10^{-4}t$ and obtained $\alpha = 0.24$. In the inset we then show our two proposed tests to estimate $T_K^{\max*}$. We see that the the D_{KS} statistics

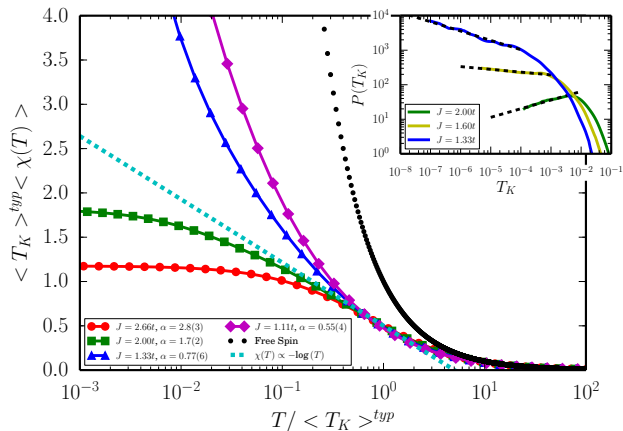


Figure S7: Icosahedral tiling. Averaged value of the impurity susceptibility $\langle \chi(T) \rangle$ times the typical value of the Kondo temperature T_K^{typ} as a function of the temperature T normalized by T_K^{typ} for four values of the Kondo coupling J on a semi-log scale. For completeness, we show both the free spin and the $\chi \propto -\log(T)$ ($\alpha = 0$) curves. Inset: Distribution of the local Kondo temperatures $P(T_K)$ as a function of T_K on a log-log scale for three values of the Kondo coupling J . J increases from the top to the bottom curve. At low T_K this distribution acquires a power-law form $P(T_K) \sim T_K^{\alpha-1}$. The power-law exponent α continuously varies with the coupling J and for $\alpha < 1$ we have a singular distribution. Here we considered $\mu = -3.0t$, $N_a = 576$, and $N_\phi = 512$.

has a minimum around $T_K^{\max} = 10^{-4}t$ and that in this region α is essentially flat as a function of T_K^{\max} , with a value of $\alpha = 0.22 \pm 0.03$.

VII. DIFFERENT TILINGS

So far we have investigated the single-impurity Kondo effect in the octagonal tiling, a $2D$ quasicrystal, while the original motivation came from experiments on a $3D$ heavy fermion quasicrystal $\text{Au}_{51}\text{Al}_{34}\text{Yb}_{15}$,^{21,24}. In the following we show that this difference in spatial dimensionality does not change the qualitative behavior of

Kondo impurities. First we note that the importance of spatial dimensionality in determining the statistics of wavefunction amplitudes (e.g. the local density of states statistics) is well known in disordered systems.²⁵ For this problem, $2D$ and $3D$ are significantly different because $2D$ is the lower critical dimension for Anderson localization.²⁶ Second, however, it is known that some models for low-dimensional (even $1D$) quasicrystals can support extended or pseudo-extended electronic states, and even a sharp Anderson-like transition and a mobility edge.²⁷ In this sense, $2D$ is most likely *not* the lower critical dimension for wavefunction localization in quasicrystals. Hence, there should not be a significant qualitative difference between electronic quasicrystalline states in $2D$ and $3D$.⁶ Therefore we expect that our $2D$ results capture the key effects of the quasicrystalline wavefunctions on the Kondo effect in general, and that our conclusions should remain valid in $3D$ thus providing a robust and general scenario for the emergence of NFL behavior in quasicrystals.

To support the claim that our results are general and applicable to different tilings (even to $3D$ quasicrystals), we have studied the Kondo problem in the $3D$ icosahedral tiling.²⁸ This tiling possesses 7 distinct local environments with coordination number $z = 4, \dots, 9$, and 12 . The average coordination number is 6 and the bandwidth is comparable to that of the simple cubic lattice. Sample results are presented in Fig. S7. As in the octagonal tiling, we obtain a power-law distribution of Kondo temperatures, $P(T_K) \sim T_K^{\alpha-1}$, and the corresponding NFL behavior for $\alpha < 1$. As discussed in the main text, the essential ingredient for this behavior is the unanticipated Gaussian form of the local c -electron cavity function fluctuations at the Fermi level, $\delta\Delta'_c$, and not any special lattice symmetry or dimension.

In conclusion, the striking similarity of our results for the octagonal and icosahedral tilings shows that NFL behavior from dilute Kondo impurities in quasicrystals is robust and serves as a starting point to understand quasicrystalline Kondo lattices, in order to connect to the recently observed NFL behavior in the $3D$ heavy fermion quasicrystal $\text{Au}_{51}\text{Al}_{34}\text{Yb}_{15}$.^{21,24}

¹ M. Kohmoto, B. Sutherland, and C. Tang, Phys. Rev. B **35**, 1020 (1987).

² A. Chhabra and R. V. Jensen, Phys. Rev. Lett. **62**, 1327 (1989).

³ A. Richardella, P. Roushan, S. Mack, B. Zhou, D. A. Huse, D. D. Awschalom, and A. Yazdani, Science **327**, 665 (2010).

⁴ A. Rodriguez, L. J. Vasquez, K. Slevin, and R. A. Römer, Phys. Rev. Lett. **105**, 046403 (2010).

⁵ A. Jagannathan and F. Piéchon, Philos. Mag. **87**, 2389 (2007).

⁶ U. Grimm and M. Schreiber, in *Quasicrystals - Structure and Physical Properties*, edited by H.-R. Trebin (Wiley-

VCH, Weinheim, 2003), pp. 210–235.

⁷ A. D. Mirlin, Phys. Rep. **326**, 259 (2000).

⁸ G. Schubert, J. Schleede, K. Byczuk, H. Fehske, and D. Vollhardt, Phys. Rev. B **81**, 155106 (2010).

⁹ C. Gros, Phys. Rev. B **53**, 6865 (1996).

¹⁰ F. F. Assaad, in *Quantum Simulations of Complex Many-Body Systems: From Theory to Algorithms*, edited by J. Grotendorst, D. Marx, and A. Muramatsu ((John von Neumann Institute for Computing (NIC), 2002).

¹¹ William H. Press *et al.*, *Numerical Recipes: The Art of Scientific Computing* (Cambridge University Press, 2007), 3rd ed.

¹² D. Tanasković, E. Miranda, and V. Dobrosavljević, Phys.

- Rev. B **70**, 205108 (2004).
- ¹³ A. Jagannathan, Phys. Rev. B **61**, R834 (2000).
- ¹⁴ A. C. Hewson, *The Kondo Problem to Heavy Fermions* (Cambridge University Press, Cambridge, 1993), 1st ed.
- ¹⁵ D. S. Fisher, Phys. Rev. B **51**, 6411 (1995).
- ¹⁶ E. Miranda and V. Dobrosavljević, Rep. Prog. Phys. **68**, 2337 (2005).
- ¹⁷ T. Vojta, J. Phys. A: Math. Gen. **39**, R143 (2006).
- ¹⁸ T. Vojta, J. Low Temp. Phys. **161**, 299 (2010).
- ¹⁹ E. Miranda, V. Dobrosavljević, and G. Kotliar, J. Phys. Cond. Mat **8**, 9871 (1996).
- ²⁰ E. Miranda, V. Dobrosavljević, and G. Kotliar, Phys. Rev. Lett. **78**, 290 (1997).
- ²¹ K. Deguchi, S. Matsukawa, N. K. Sato, T. Hattori, K. Ishida, H. Takakura, and T. Ishimasa, Nat. Mater. **11**, 1013 (2012).
- ²² H. Q. Yuan, U. Grimm, P. Repetowicz, and M. Schreiber, Phys. Rev. B **62**, 15569 (2000).
- ²³ A. Clauset, C. R. Shalizi, and M. E. J. Newman, SIAM Review **51**, 661 (2009).
- ²⁴ T. Watanuki, S. Kashimoto, D. Kawana, T. Yamazaki, A. Machida, Y. Tanaka, and T. J. Sato, Phys. Rev. B **86**, 094201 (2012).
- ²⁵ P. W. Anderson, Phys. Rev. **109**, 1492 (1958).
- ²⁶ E. Abrahams, P. W. Anderson, D. C. Licciardello, and T. V. Ramakrishnan, Phys. Rev. Lett. **42**, 673 (1979).
- ²⁷ J. Luck and D. Petritis, J. Stat. Phys. **42**, 289 (1986).
- ²⁸ E. S. Zijlstra and T. Janssen, Europhys. Lett. **52**, 578 (2000).